# High Gain Bismuth-Doped Fiber Amplifier Operating in the E+S Band with Record Gain per Unit Length

Ziwei Zhai, Arindam Halder, and Jayanta K. Sahu

***Abstract*—We experimentally demonstrate high-gain E+S band bismuth (Bi)-doped fiber amplifiers (BDFAs) using Bi-doped germanosilicate fiber (BGSF) with lengths shorter than those widely reported in the literature, ranging from 25.5 to 48m. In a double-pass amplifier configuration, a 39.9dB gain with 5.6dB noise figure (NF) is achieved at 1440nm using 35m of BGSF, for a -23dBm input signal. By reducing the fiber length to 25.5m, we achieve the highest recorded gain per unit length of 1.33dB/m, to the best of our knowledge, with 33.8dB gain and 3.7dB NF for an input signal of -23dBm. The highest power-conversion-efficiency (PCE) is 18.3%, obtained by 48m of BGSF using 375mW pump power and -10dBm signal power. From 1410-1490nm, the in-band optical signal-to-noise ratio (OSNR) is >21dB for a -23dBm input signal and >33dB for a -10dBm input signal. The temperature-dependent gain is characterized from -60 to 80ºC, with the longer BGSF length exhibiting better thermal stability. Moreover, three BGSFs with an increasing $GeO_2$ concentration, measured to be in the range of 3.7-16mol%, are studied in detail for their absorption and luminescence characteristics. An absorption band peaking at ~1370nm has appeared and is likely to be associated with the bismuth-active-center (BAC) connected to the Ge, BAC-Ge. By increasing the $GeO_2$ concentration to 16mol%, the 1370nm BAC-Ge absorption band starts to dominate over the 1405nm BAC-Si absorption band, while simultaneously the other BAC-Ge absorption band at 1640nm appears. The luminescence exhibits a wider bandwidth with an increase in $GeO_2$ content, favoring the E+S band amplification.**

***Index Terms*— Bismuth, doped fiber amplifiers, optical fibers, germanosilicate fibers**

## I. Introduction

A higher data-carrying capacity of optical fibers is required to support the increasing demand for bandwidth-intensive applications in modern networks, such as virtual reality (VR) and augmented reality (AR), cloud-based services, big data processing, ultra-high definition videos, etc. As an emerging technology in optical communications, bismuth (Bi)-doped fiber amplifiers (BDFAs) have been recognized as a research hotspot to expand the data transmission bandwidth. As a promising active gain medium, Bi-doped fiber (BDF) exhibits an ultra-wide near-infrared (NIR) luminescence covering O, E, S, and U bands by tailoring the glass composition and forming various Bi active centers (BACs). With no efficient rare earth-doped fiber amplifiers available in the wavelength region of 1150-1500 nm and ~1700 nm, BDFAs can provide amplification in these bands, using aluminosilicate fibers to amplify the signal at ~1180 nm [1], phosphosilicate fibers to cover 1280-1460 nm [2], [3], [4], [5], [6], germanosilicate fibers to cover 1370-1500 nm [7], [8], [9], and high germanosilicate (≥50 mol% of $GeO_2$) fibers to go beyond 1640 nm [10]. The highest gain of BDFAs reported to date is ~40 dB in O- [2] and E- [4, 8] bands for a -23 dBm input signal. A detailed review of BDFAs can be found in [11].

However, it is still poorly understood on the properties of various BACs and their corresponding contribution to the NIR absorption and luminescence, which determine the effective pump and signal wavelengths for efficient operation of the amplifier. The development of BDFAs has a critical challenge in balancing the Bi concentration, states and concentrations of the host glass composition dependent BACs, and their dominant luminescence bands. Unfortunately, a slightly higher Bi concentration might induce a significant increase in the unsaturable loss and background loss, thus resulting in poor amplification performance. Accordingly, the current generation of BDFAs usually has a low Bi concentration of ≤0.1 mol%, where a long fiber length of hundreds of meters is required to achieve sufficient gain [11]. In the O-band, the maximum gain per unit length of 0.48 dB/m from a double-pass BDFA is reported using 65 m of Bi-doped phosphosilicate fiber (BPSF), where a maximum gain of 30 dB with 7 dB NF is reported [6]. In the E+S band, we have demonstrated a double-pass BDFA providing 38 dB maximum gain with 6.9 dB NF at 1455 nm using 250 m of Bi-doped germanosilicate fiber (BGSF), where the gain per unit length is 0.152 dB/m [8]. We recently report a single-pass BDFA using 35 m of BGSF with a maximum gain of 23 dB with 4.1 dB NF at 1440 nm, where the gain per unit length has significantly increased to 0.66 dB/m [9]. We also reported on a double-pass BDFA operating in the E+S band, providing ~40 dB gain and ≥1.14 dB gain per unit length when using 35 m of BGSF [12].

In this paper, we extend our study to the absorption and

This paragraph of the first footnote will contain the date on which you submitted your paper for review. This work was supported by the Engineering and Physical Sciences Research Council, U.K. under Grant EP/P030181/1. *(Corresponding author: Ziwei Zhai.)*

The authors are with Optoelectronics Research Centre, University of Southampton, Southampton, SO17 1BJ, U.K. (e-mail: z.zhai@soton.ac.uk; a.halder@soton.ac.uk; jks@orc.soton.ac.uk).

TABLE I
BASIC CHARACTERISTICS OF BGSFS IN THIS WORK

| | dn | $GeO_2$ (mol%) | Core/cladding diameter (μm) | Abs@1304nm (dB/m) | Abs@1333nm (dB/m) | Abs@1385nm (dB/m) | UL@1333nm | BL@1100nm (dB/m) |
|---|---|---|---|---|---|---|---|---|
| BGSF-1 | 0.022 | 16 | 3.6/125 | 1.15 | 1.69 | 3.8 | 15% | 0.15 |
| BGSF-2 | 0.01 | 8.1 | 6.1/100 | 0.21 | 0.33 | 1.4 | 22% | 0.036 |
| BGSF-3 | 0.0048 | 3.7 | 8/125 | 0.16 | 0.26 | 1.34 | 37% | 0.06 |

luminescence properties of BGSFs with different $GeO_2$ concentrations measured to be in the range of 3.7-16 mol%. BGSF-1, with a $GeO_2$ concentration of 16 mol%, demonstrates a higher Bi concentration and/or a larger fraction of effective BAC sites, as indicated by the absorption around pump wavelengths, that favor Bi luminescence in the E+S band while maintaining well-controlled unsaturable loss in fiber. The absorption is found to include both BAC-Si and BAC-Ge bands, where a new absorption band peaking at ~1370 nm is expected to be associated with BAC-Ge. An effective pump wavelength region of 1304-1333 nm is selected to develop the amplifier in the E+S band. We have demonstrated a double-pass BDFA using a 35 m length of BGSF-1, providing 39.9 dB gain with 1.14 dB gain per unit length at 1440 nm for a -23 dBm input signal. By further reducing the length to 25.5 m, the gain per unit length is increased to 1.42 dB/m for a small-signal of -30 dBm, which is the highest gain per unit length reported to date, to the best of our knowledge. In addition, the noise figure (NF), 3-dB bandwidth, gain coefficient, pump-to-signal power conversion efficiency (PCE), in-band optical signal-to-noise ratio (OSNR), and temperature-dependent gain (TDG) coefficient are reported for different lengths of BGSF used in the amplifier.

## II. BI-DOPED GERMANOSILICATE FIBER CHARACTERIZATION

A series of Bi-doped germanosilicate preforms were fabricated in-house using the modified chemical vapor deposition (MCVD) and solution doping technique, then drawn into fibers at a temperature of ~2000 ºC using a drawing speed of ~10 m/min. By tailoring the glass composition, adjusting the dopant concentration in the solution, and refining the fabrication conditions, three BGSFs are selected to study with a different $GeO_2$ concentration measured to be 16 mol% for BGSF-1, 8.1 mol% for BGSF-2, and 3.7 mol% for BGSF-3. The $GeO_2$ concentration was measured by the electron probe microanalyzer (EPMA). The refractive index difference (dn) profile was measured using the optical fiber refractive index profiler (IFA-100, Interfiber Analysis), where the dn is 0.022 for BGSF-1, 0.01 for BGSF-2, and 0.0048 for BGSF-3, as shown in the inset of Fig. 1. The absorption spectra are measured by the cut-back method using a white light source (IL1, Bentham), as shown in Fig. 1. The absorption at the pump wavelengths of 1304 and 1333 nm and the unsaturable loss (UL) at 1333 nm are presented in Table I, with the absorption peak at ~1385nm to be 3.8 dB/m for BGSF-1, 1.4 dB/m for BGSF-2, and 1.34 dB/m for BGSF-3. The background loss (BL) measured at 1100 nm is 0.15, 0.036, and 0.06 dB/m for BGSF-1, BGSF-2, and BGSF-3, respectively.

The luminescence of the BGSF is measured using the experimental setup shown in Fig. 2(a), where a 3 m piece of BGSF is pumped by a laser diode (LD) at 1333 nm with a 5 mW power. The luminescence spectrum is captured from the pump launch end, using an optical spectrum analyzer (OSA, AQ6370, YOKOGAWA) with a resolution bandwidth of 1 nm. The background noise from the pump light has been subtracted from the measured spectrum.

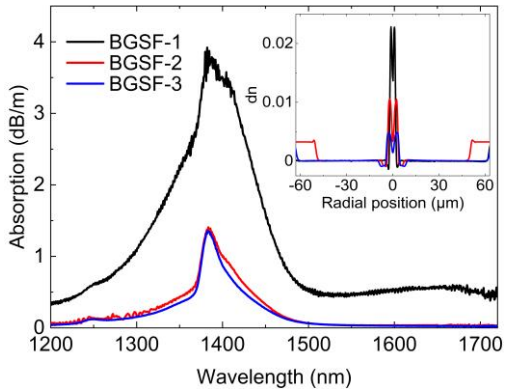


Fig. 1. Absorption spectra of BGSF-1, BGSF-2, and BGSF-3 (the inset represents the refractive index difference profiles).

The gain and noise figure (NF) spectra of the BGSF are characterized in a double-pass E+S band BDFA experimental setup, as shown in Fig. 2(b). The splice loss between the BGSFs and the conventional SMF-28 used in the setup was measured to be 0.89 dB for BGSF-1, 0.37 dB for BGSF-2, and 0.08 dB for BGSF-3 at the signal wavelengths. The BGSF is bi-directionally pumped by three laser diodes (LDs), including one 1333 nm LD and two LDs combined by a polarization beam

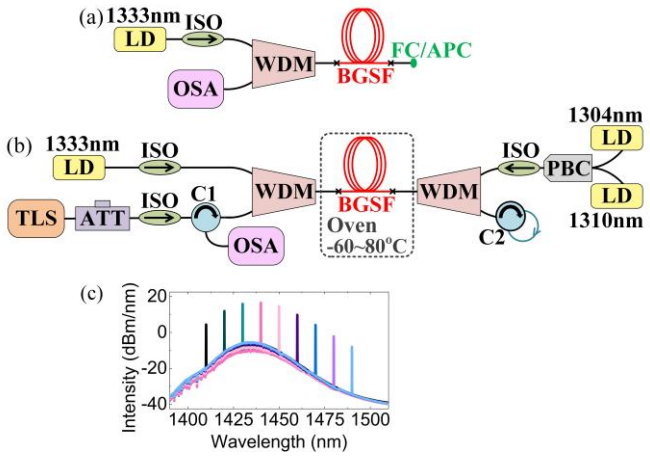


Fig. 2. (a) Experimental schematic of the Bi luminescence measurement. (b) Experimental schematic of the double-pass E+S band BDFA. (c) The output signal and ASE spectra of 35 m of BGSF-1 for a -23 dBm input signal from which the in-band OSNR is derived.

combiner (PBC), operating at 1304 and 1310 nm, respectively. A tunable laser source (TLS) with a linewidth of 400 kHz is used as the signal source, followed by an attenuator (ATT). Isolators (ISO) are used to protect the components and two wavelength division multiplexers (WDMs) are used to couple and separate the pump and signal lights. An OSA is used to record the input and output signals, using a resolution bandwidth of 0.2 nm. Fig. 2(c) shows the output signal and amplified spontaneous emission (ASE) spectra measured for 35 m of BGSF-1 at room temperature (RT) using a -23 dBm input signal, where the in-band OSNR is derived. Considering the splice loss between the BGSF and the commercial SMF28 used in the setup, the input signal spectrum is measured after a short piece of BGSF (<0.1m) spliced to the WDM. To efficiently utilize the amplification media and enhance the gain, a double-pass amplifier configuration is used by applying two circulators (C1 and C2). The circulator loss was measured to be 1.05±0.49 dB from 1400-1500 nm. Moreover, a thermal oven operating from -60 to 80 °C is used to characterize the temperature-dependent gain with the BGSF placed inside and a thermometer is used to monitor the temperature of the fiber surface. The gain and NF (in the unit of dB) are calculated based on the measured input and output signal spectra, described by (1)-(3).

$$G_{dB} = 10log_{10}\left(\frac{P_{out} - N_{out}}{P_{in}}\right) \quad (1)$$

$$NF_{dB} = 10log_{10}\left(\frac{\lambda}{hcB_0}\frac{N_{out} - N_{in}G_{linear}}{G_{linear}} + \frac{1}{G_{linear}}\right) \quad (2)$$

$$B_0 = \frac{c\,\Delta\lambda_{OSA}}{\lambda^2} \quad (3)$$

In which, $P_{in}$ and $P_{out}$ are the input and output power (in the unit of W) at the signal wavelength, respectively. $B_0$ is the frequency spacing of OSA resolution (in the unit of Hz). $N_{in}$ and $N_{out}$ are the input and output noise power (in the unit of W), respectively. The noise power intensity is chosen from the measured spectrum at ~1.5 nm adjacent to the signal wavelength. $G_{linear}$ represents the gain in the linear unit.

## III. Results and Discussion

### A. Absorption of Bi-doped germanosilicate fibers

Fig. 3 shows the normalized absorption spectra of three BGSFs after subtracting the background loss. The normalized absorption is fitted to multiple Gaussian bands, contributed from the OH groups and BACs associated with Ge (BAC-Ge) and Si (BAC-Si) in the glass matrix. The peak amplitude of each band is presented in the graph. The 1385 nm absorption band is induced by the OH content, with a narrow FWHM (full width at half maximum) of 15-18 nm for the three BGSFs. The absorption band peaking at ~1405 nm is associated with BAC-Si [13] with subtle difference in the three BGSFs. The peak amplitude is 0.44, 0.46, and 0.38 for BGSF-1, BGSF-2, and BGSF-3, respectively. The FWHM is 70, 66, and 63 nm for BGSF-1, BGSF-2, and BGSF-3, respectively.

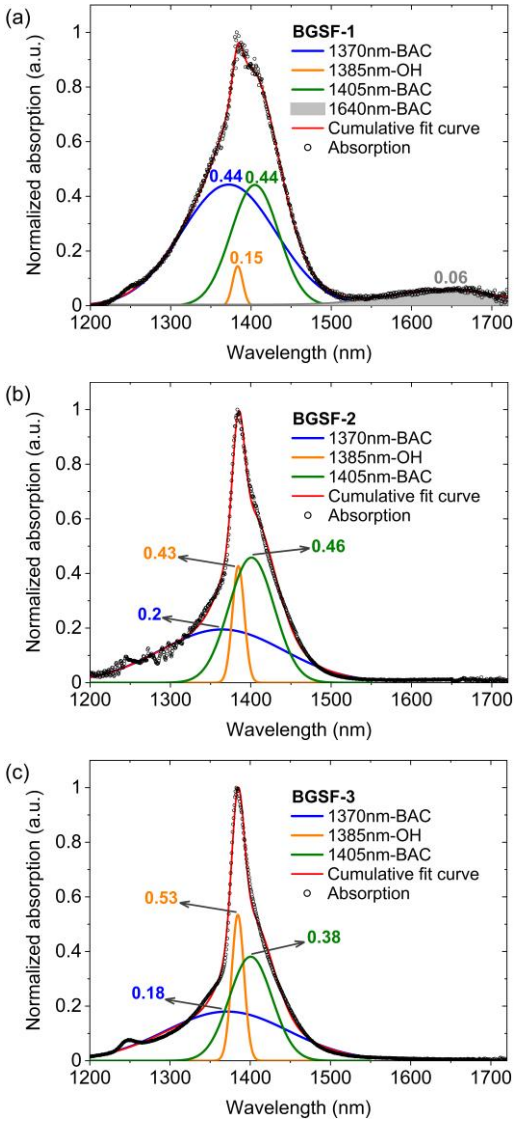


Fig. 3. Gaussian peaks fittings to the normalized absorption curve after subtracting the background loss for (a) BGSF-1, (b) BGSF-2, and (c) BGSF-3.

The influence of $GeO_2$ content on the presence of BACs in the BGSF is observed in the 1370 nm-BAC band and 1640 nm-BAC band. The 1370 nm absorption band exhibits a similar amplitude (~0.2) and FWHM (~180 nm) for BGSF-2 and BGSF-3, with a $GeO_2$ content of 8.1 and 3.7 mol%, respectively. While for BGSF-1, containing a higher $GeO_2$ content of 16 mol%, the amplitude of the 1370 nm absorption band increases to 0.44 with a narrower FWHM (138 nm). In addition, a distinct absorption band appears at 1640 nm for BGSF-1, which has been studied to be related to BAC-Ge and is absent for low $GeO_2$ concentrations [14], [15]. Considering the difference of the 1370 nm-BAC band in low and high $GeO_2$ concentrations, we strongly believe that it is related to BAC-Ge. Moreover, the ratio of the amplitude of 1370 nm-BAC to the amplitude of 1405 nm-BAC is more than doubled from BGSF-2 and BGSF-3 to BGSF-1. It is observed that the 1370 nm-BAC starts to dominate as the $GeO_2$ concentration increases to 16 mol% in BGSF-1, where the same amplitude of 0.44 is observed for 1370 nm-BAC and 1405 nm-BAC. By further increasing the $GeO_2$ concentration, the amplitudes of the 1370

nm-BAC and 1640 nm-BAC simultaneously increase and the 1640 nm-BAC gradually starts to dominate, which is no longer favoring the gain in the E+S band thus going beyond the scope of this study. Additionally, the contribution from BAC-Si to the 1370 nm-BAC band cannot be fully ruled out, given that a ~1335 nm absorption band was reported in pure $SiO_2$ fiber [13].

It is worth mentioning that the wavelength range of 1300-1360 nm represents a potential pump region to consider for the E+S-band BDFA, as BGSFs exhibit a broad absorption spectrum within this range without overlapping the 1385 nm OH absorption band.

### *B. Luminescence and gain of Bi-doped germanosilicate fibers*

Fig. 4 shows the luminescence intensity spectra pumped at 1333 nm of the three BGSFs, where the inset shows the normalized luminescence intensity. The luminescence intensity increases from BGSF-3 to BGSF-2 and is significantly improved for BGSF-1. The normalized intensity is similar for BGSF-2 and BGSF-3, while BGSF-1 exhibits a wide 3-dB bandwidth of 134 nm, which is ~16 nm wider than that of BGSF-2 and BGSF-3. The peak wavelength slightly red-shifts with an increasing $GeO_2$, which is 1416 nm for BGSF-3, 1422 nm for BGSF-2, and 1425 nm for BGSF-1. Such luminescence difference is expected to be the influence of $GeO_2$, as reported that the BAC-Ge luminescence spectrum shifts a little towards longer wavelengths compared to that of BAC-Si luminescence [16]. The pump wavelength of 1304 nm is also used for the luminescence measurement and there is only a slight increase in the intensity below 1415 nm compared to the results pumped at 1333 nm.

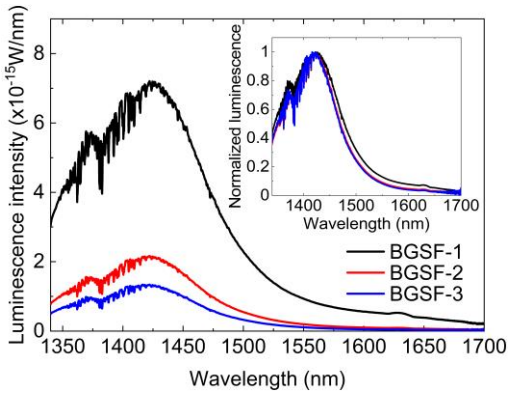


Fig. 4. Luminescence spectra of BGSF-1, BGSF-2, and BGSF-3 (the inset represents the normalized luminescence intensity).

Among the three BGSFs, BGSF-3 exhibits the lowest Bi absorption of 0.26 dB/m at 1333 nm, while the absorption at 1333 nm is 0.33 dB/m for BGSF-2 and increases to 1.69 dB/m for BGSF-1. However, the unsaturable loss (UL) at 1333 nm is 37% for BGSF-3, much higher than a 22% UL for BGSF-2 and 15% UL for BGSF-1. Also considering the lowest luminescence intensity, BGSF-3 is believed to have a low Bi concentration and/or a low fraction of effective BAC states. Since the spectroscopic properties of absorption and luminescence are similar for BGSF-2 and BGSF-3, BGSF-2 is selected for further amplifier characterizations to compare with BGSF-1, which exhibits a high BAC concentration and wider luminescence in the E+S band.

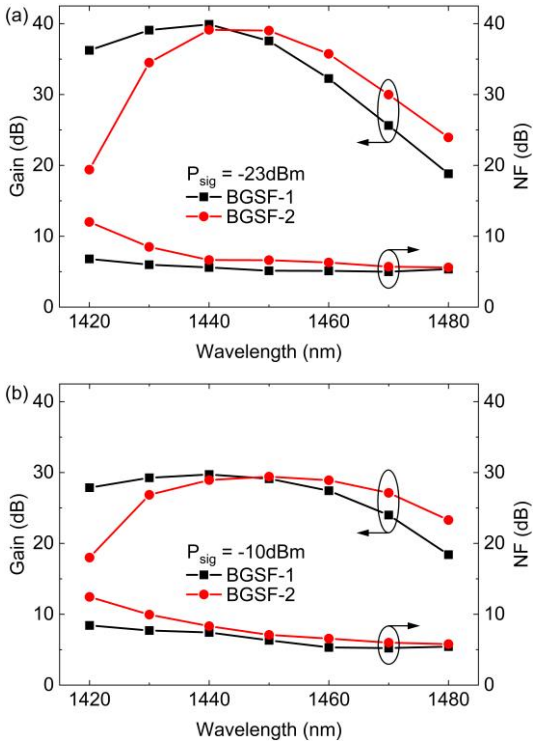


Fig. 5. Gain and NF spectra of BGSF-1 and BGSF-2 from 1420-1480 nm for an input signal power of (a) -23 dBm and (b) -10 dBm at RT ($P_{pump}$ = 681 mW; BGSF-1: L = 35 m; BGSF-2: L = 150 m).

BGSF-1 and BGSF-2 are tested in the E+S band BDFA at room temperature (RT), for an input signal power of -23 and -10 dBm, respectively. The total pump power launched into the BGSF is 681 mW, i.e., 325 mW from 1333 nm LD and 356 mW from 1304+1310 nm LDs. Fig. 5 shows the gain and NF spectra from 1420-1480 nm using a 35 m length of BGSF-1 and a 150 m length of BGSF-2, respectively. The fiber length is optimized with respect to a higher gain (reaching close to 40 dB at 1440 nm for a -23 dBm input signal) and a wider 3-dB bandwidth. For a -23 dBm input signal, we achieve a maximum 39.9 dB gain with 5.6 dB NF for BGSF-1 at 1440 nm, where BGSF-2 has a 39.1 dB gain with 6.6 dB NF. The 3-dB bandwidth is 30.5 nm for BGSF-1 and 25 nm for BGSF-2. For a -10 dBm input signal, we achieve a 29.7 dB gain with 7.4 dB NF for BGSF-1 and a 28.9 dB gain with 8.3 dB NF for BGSF-2 at 1440 nm. The 3-dB bandwidth is 46 nm for BGSF-1 and 42 nm for BGSF-2. Both BGSF-1 and BGSF-2 can achieve a high gain, which is close to 40 dB for a -23 dBm input signal and close to 30 dB for a -10 dBm input signal at 1440 nm. A wider 3-dB bandwidth for BGSF-1 is attributed to its wider luminescence band. Critically, the NF of BGSF-1 is lower, thanks to its shorter device length. As discussed in Section A, the 1370 nm-BAC is more dominant in BGSF-1 than in BGSF-2, contributing to a more effective pump absorption at the wavelength region of 1304-1333 nm to obtain the gain in the E+S band. Also, the Bi absorption of BGSF-1 at the pump wavelengths is more than 5 times the Bi absorption of BGSF-2. Accordingly, the device length is significantly reduced to 35 m for BGSF-1, achieving a much higher gain per unit length of 1.14 dB/m at 1440 nm for

TABLE II
AMPLIFIER CHARACTERISTICS OF BGSF-1 USING DIFFERENT FIBER LENGTHS IN THIS WORK

| $P_{sig}$ (dBm) | Length (m) | $\lambda_{sig}$ = 1440 nm | | | | | | 3-dB bandwidth (nm) | TDG coefficient (dB/°C) |
|---|---|---|---|---|---|---|---|---|---|
| | | Gain (dB) | Gain per unit length (dB/m) | Gain coefficient (dB/mW) | PCE | NF (dB) | In-band OSNR (dB) | | |
| -23 | 48 | **40.5** | 0.84 | 0.319 | **11.4%** | 6.3 | 25.7 | 26 | **-0.018~0.014** |
| | 35 | 39.9 | 1.14 | **0.458** | 7% | 5.6 | 26.9 | **30.5** | -0.024~0.014 |
| | 30 | 37.2 | 1.24 | 0.445 | 3.7% | 4.7 | 28.2 | 30 | -0.055~0.008 |
| | 25.5 | 33.8 | **1.33** | 0.37 | 1.8% | **3.7** | **29** | 30 | -0.077~0 |
| -10 | 48 | 29.3 | 0.61 | 0.194 | **17.9%** | 8.3 | 37.9 | 43.5 | **-0.005~0.014** |
| | 35 | **29.7** | 0.85 | **0.298** | 13.8% | 7.4 | 38.1 | **46** | -0.019~0.014 |
| | 30 | 28.5 | 0.95 | 0.295 | 10.5% | 5.9 | 39.6 | 42 | -0.031~0.009 |
| | 25.5 | 26.3 | **1.03** | 0.246 | 6.2% | **5.3** | **40.2** | 40.5 | -0.046~0.003 |

a -23 dBm input signal, compared to 0.26 dB/m for BGSF-2. A lower UL for BGSF-1 also helps reduce the NF and increase the pump efficiency. The pump-to-signal power conversion efficiency (PCE) is found to be 13.8% for BGSF-1 and 11.6% for BGSF-2 at 1440 nm for a -10 dBm input signal.

### *C. E+S band amplifier with a high gain per unit length*

Benefiting from a short fiber length of only 35 m in the E+S band amplifier, a detailed study on BGSF-1 is performed in terms of different fiber lengths, pump and signal powers, and temperatures. Fig. 6 shows the gain and NF spectra from 1410-1490 nm using different lengths of BGSF-1 (48, 35, 30, and 25.5 m) measured at RT for an input signal of -23 and -10 dBm, respectively. The total pump power is 475 mW for 48 m of BGSF-1 and 681 mW for 35, 30, and 25.5 m of BGSF-1, optimized in terms of a high gain and high PCE at 1440 nm. Table II presents the amplifier characteristics using 48, 35, 30, and 25.5 m of BGSF-1, where the highlights with bold and underlined font represent the best-performing parameters using the corresponding fiber length. Using a 48 m of BGSF-1, a lower pump power of 475 mW is enough to achieve >40 dB gain at 1440 nm for a -23 dBm input signal, together with a high PCE of 11.4%. For a -10 dBm input signal, the gain is 29.3 dB with 17.9% PCE at 1440 nm. By decreasing the fiber length, although the gain decreases, the gain per unit length increases to 1.33 dB/m for a -23 dBm signal and 1.03 dB/m for a -10 dBm signal using 25.5 m of fiber. Also, the NF significantly improves to be 3.7 dB for a -23 dBm signal and 5.3 dB for a -10 dBm signal, with a compromised performance of the PCE. In all the circumstances, the in-band OSNR is >21 dB for a -23 dBm signal and >33 dB for a -10 dBm signal from 1410-1490 nm.

Then, we measure the gain and NF variations with the pump power (maximum 681 mW) for 48 to 25.5 m of BGSF-1 at 1440 nm, as Fig. 7 shows. The gain coefficient is calculated as the maximum ratio of the gain to the pump power. The highest gain coefficient at 1440 nm is achieved for 35 m of BGSF, which is 0.458 dB/mW for a -23 dBm input signal and 0.298 dB/mW for a -10 dBm input signal.

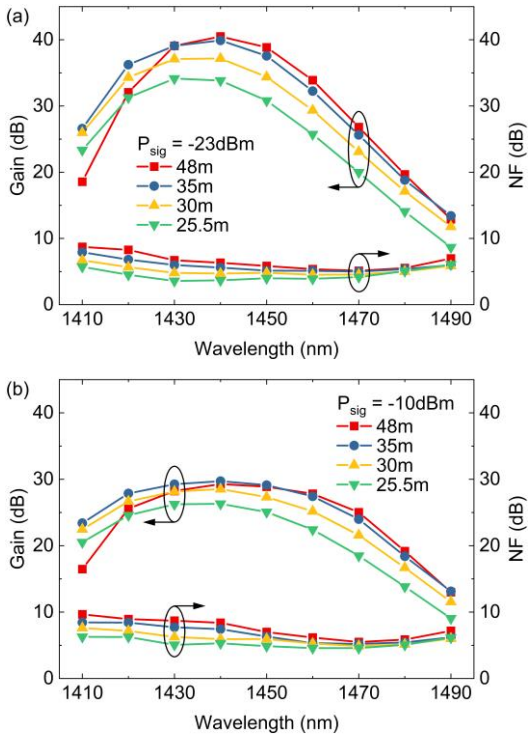


Fig. 6. Gain and NF spectra from 1410-1490 nm using 48, 35, 30, and 25.5 m of BGSF-1, for an input signal power of (a) -23 dBm and (b) -10 dBm at RT ($P_{pump}$= 475 mW for L= 48 m; $P_{pump}$= 681 mW for L= 35, 30, and 25.5 m).

Next, we measure the gain and NF variations with the input signal power at 1440 nm, as Fig. 8 shows. For a small-signal of -30 dBm, 36.2 dB gain with 3.6 dB NF is achieved using 25.5 m of BGSF-1. The gain per unit length is 1.42 dB/m, which is, to the best of our knowledge, a record value reported for BDFAs. For a 0 dBm input signal, we achieve >18 dB gain using different lengths of BGSF-1. Fig. 9 shows the relation between the PCE and the pump and signal powers at 1440 nm using different fiber lengths. The highest PCE is 18.3%, achieved for a 375 mW pump power and -10 dBm input signal using 48 m of BGSF-1. The highest PCE was obtained by optimizing the fiber length and pump power to fully utilize the pump energy meanwhile minimizing the generation of

excessive ASE.

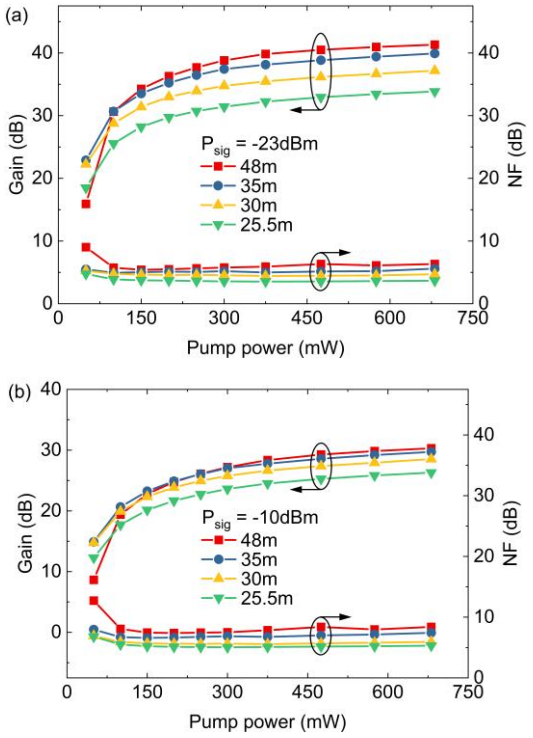


Fig. 7. Gain and NF variations with the pump power (maximum 681 mW) at 1440 nm using 48, 35, 30, and 25.5 m of BGSF-1 at RT, for an input signal power of (a) -23 dBm and (b) -10 dBm.

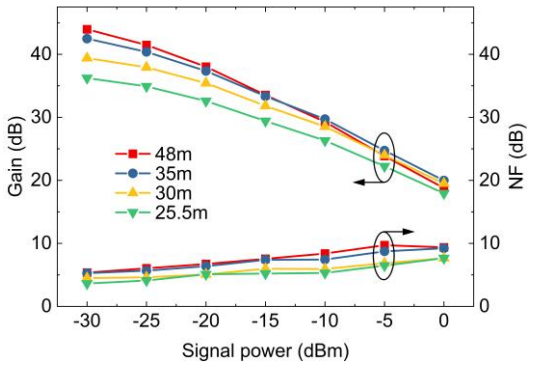


Fig. 8. Gain and NF variations with the input signal power at 1440 nm using 48, 35, 30, and 25.5 m of BGSF-1 at RT ($P_{pump}$ = 475 mW for L = 48 m; $P_{pump}$ = 681 mW for L = 35, 30, and 25.5 m).

Furthermore, we measure the temperature-dependent gain performance of BGSF-1 from -60 to 80 ºC and calculate the temperature-dependent gain (TDG) coefficient as the gain change per unit temperature change. Fig. 10 shows the TDG coefficient spectra using different fiber lengths. The temperature stability improves with an increasing fiber length, with a TDG coefficient in the range of -0.018 to 0.014 dB/ºC for a -23 dBm signal and -0.005 to 0.014 dB/ºC for a -10 dBm signal using 48 m of BGSF-1. The TDG performance is similar to that of EDFAs [17]. The reported BGSF-1 provides flexible choices for customizing the amplifier parameters considering the specific requirements of the applications, including the gain, NF, 3-dB bandwidth, efficiency, and temperature stability.

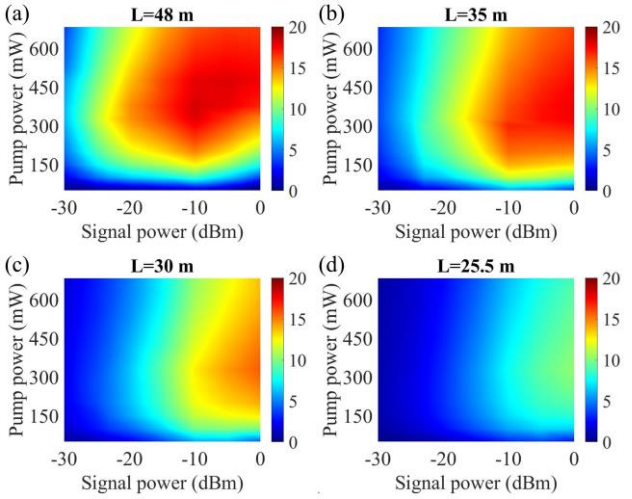


Fig. 9. PCE (in the unit of %) color map against the pump and signal powers using (a) 48 m, (b) 35 m, (c) 30 m, and (d) 25.5 m of BGSF-1 at RT.

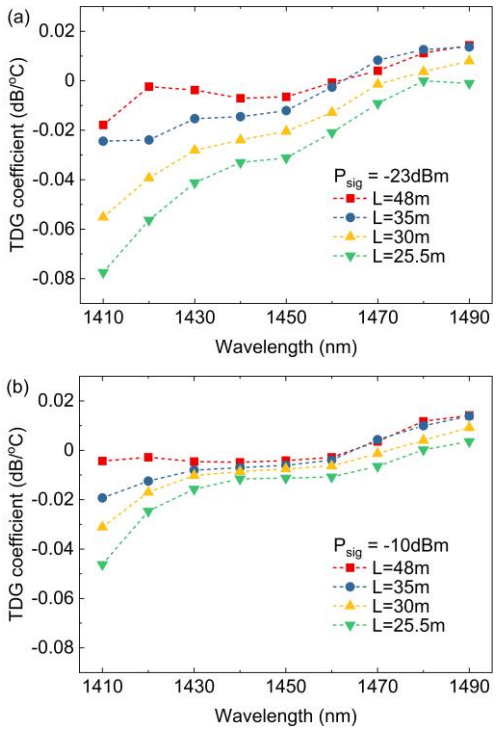


Fig. 10. TDG coefficient spectra from 1410-1490 nm using 48, 35, 30, and 25.5 m of BGSF-1, for an input signal power of (a) -23 dBm and (b) -10 dBm ($P_{pump}$ = 475 mW for L = 48 m; $P_{pump}$ = 681 mW for L = 35, 30, 25.5 m).

### *D. Measurement uncertainty of gain and noise figure*

To evaluate the measurement errors of the amplifier in this work, we derive the gain and NF uncertainty using the equation described by (4). In which, Y is a function of $x_i$, i.e., $Y = Y(x_i)$, where i = 1, 2, …, n. $\delta Y$ and $\delta x_i$ represent the measurement uncertainty of Y and $x_i$, respectively. n value is 30 in this work.

$$\pm\delta Y = \pm\sqrt{\sum_{i=1}^{n}\left(\frac{\partial Y}{\partial x_i}\right)^2(\delta x_i)^2} \tag{4}$$

The measurement uncertainty of the gain (in the dB unit) is derived from (1), represented by $\delta G_{dB}$ as described by (5). The

measurement uncertainty of the gain (in the linear unit) is represented by $\delta G_{linear}$ as described by (6).

$$\pm\delta G_{dB} = \pm\sqrt{\left(\frac{10}{P_{\text{out}}\ln 10}\right)^2(\delta P_{\text{out}})^2 + \left(\frac{10}{P_{\text{in}}\ln 10}\right)^2(\delta P_{\text{in}})^2} \quad (5)$$

$$\pm\delta G_{linear} = \pm\frac{G_{\text{linear}}\ln 10}{10}\delta G_{dB} \quad (6)$$

The measurement uncertainty of the NF (in the dB unit) is derived from (2), represented by $\delta NF_{dB}$ as described by (7). The measurement uncertainty of the NF (in the linear unit) is represented by $\delta NF_{linear}$ as described by (8).

$$\pm\delta NF_{dB} = \pm\sqrt{\left(\frac{10}{N_{\text{out}}\ln 10}\right)^2(\delta N_{\text{out}})^2 + \left(\frac{10}{N_{\text{in}}\ln 10}\right)^2(\delta N_{\text{in}})^2 + \left(\frac{10}{G_{\text{linear}}\ln 10}\right)^2(\delta G_{\text{linear}})^2} \quad (7)$$

$$\pm\delta NF_{linear} = \pm\frac{NF_{\text{linear}}\ln 10}{10}\delta NF_{dB} \quad (8)$$

For BGSF-1 using different lengths, the measurement uncertainty at 1440 nm is found to be within ±0.16 dB for the gain and within ±0.33 dB for the NF. To evaluate the percentage uncertainty, the gain and NF in the linear unit are used, i.e., $\delta G_{\text{linear}}/G_{linear}$ and $\delta NF_{\text{linear}}/NF_{linear}$ . The percentage uncertainty is found to be within 3.6% for the gain and within 7.3% for the NF. In addition, it is observed that the measurement uncertainty of the NF is dominated by the percentage uncertainty of the gain (i.e., $\delta G_{\text{linear}}/G_{\text{linear}}$) and marginally affected by the percentage uncertainty of $N_{in}$ and $N_{out}$ (i.e., $\delta N_{\text{in}}/N_{\text{in}}$ and $\delta N_{\text{out}}/N_{\text{out}}$).

## IV. Conclusion

In conclusion, we fabricated BGSFs using the MCVD-solution doping technique by tailoring the glass composition and increasing the effective BAC to favor the E+S band amplification. Three BGSFs with different $GeO_2$ concentrations are characterized by the absorption bands peaking at ~1370, 1405, and 1640 nm. The 1370 nm-BAC band, likely attributed to BAC-Ge, is found to be dominant when the $GeO_2$ content increases to 16 mol% in BGSF-1. Also, the 1640 nm-BAC band (BAC-Ge) appears for BGSF-1. The luminescence intensity is characterized by a wider bandwidth in the E+S band when increasing the $GeO_2$. An effective pump wavelength region of 1304-1333 nm is used to demonstrate a double-pass BDFA in the E+S band, where different lengths of BGSF-1 are used to evaluate the pros and cons of the amplifier performance. Using 35 m of BGSF-1, a maximum gain of 39.9 dB with 5.6 dB NF is achieved at 1440 nm for a -23 dBm input signal, where the gain per unit length is 1.14 dB/m. The highest gain per unit length of 1.42 dB/m is achieved when using a 25.5 m length for a -30 dBm signal at 1440 nm, with 36.2 dB gain and 3.6 dB NF. The highest PCE of 18.3% is achieved for a -10 dBm signal using a 48 m length and 375 mW pump power. The temperature-dependent gain performance is studied from -60 to 80 °C to illustrate the thermal stability of the amplifier. The reported BDFA holds great potential in developing a compact and high-gain amplifier in the E+S band.

Based on the BGSFs reported here, further increasing the $GeO_2$ (beyond 20 mol%) promotes the 1640 nm-BAC, which gradually starts to dominate with the gain red-shifting to longer wavelengths beyond the E+S band. Such investigations are beyond the scope of this article and will be studied in our future work.

## Acknowledgment

The authors are thankful to Dr. Andrew Matzen from the Department of Earth Sciences, University of Oxford, for his valuable support and assistance with the EPMA measurement.

This work was supported by the Engineering and Physical Sciences Research Council, U.K. under Grant EP/P030181/1. Data underlying the results presented in this paper can be accessed at: https://doi.org/10.5258/SOTON/D2865.

## References

[1] N. K. Thipparapu et al., "1120 nm diode-pumped Bi-doped fiber amplifier," *Opt. Lett.*, vol. 40, no. 10, pp. 2441–2444, 2015.

[2] N. K. Thipparapu et al., "40 dB gain all fiber bismuth-doped amplifier operating in the O-band," *Opt. Lett.*, vol. 44, no. 9, pp. 2248–2251, 2019.

[3] A. Khegai et al., "O-band bismuth-doped fiber amplifier with 67 nm bandwidth," in *Proc. Opt. Fiber Commun. Conf.*, San Diego, CA, USA, 2020, Paper W1C.4.

[4] Y. Wang et al., "High gain Bi-doped fiber amplifier operating in the E-band with a 3-dB bandwidth of 40nm," in *Proc. Opt. Fiber Commun. Conf.*, Washington, DC, USA, 2021, Paper Tu1E.1.

[5] Y. Ososkov et al., "Pump-efficient flattop O+E-bands bismuth-doped fiber amplifier with 116 nm-3 dB gain bandwidth*," Opt. Exp*., vol. 29, no. 26, pp. 44138–44145, 2021.

[6] Y. Chen et al., "Near 0.5 dB gain per unit length in O-band based on a Bi/P co-doped silica fiber via atomic layer deposition," *Opt. Exp*., vol. 31, no. 9, pp. 14862–14872, 2023.

[7] A. Donodin et al., "Bismuth doped fibre amplifier operating in E- and S-optical bands," *Opt. Mater. Exp*., vol. 11, no. 1, pp. 127–135, 2021.

[8] Y. Wang, A. Halder, and J. K. Sahu, "Bi-doped fiber amplifier operating in the wavelength range of 1430-1500 nm," in *Proc. Advanced Solid State Lasers Conference (ASSL)*, Tacoma, WA, USA, 2023, Paper ATh1A.1.

[9] S. Wang et al., "Bi-doped fiber amplifiers in the E+S band with a high gain per unit length," *Opt. Lett.*, vol. 48, no. 21, pp. 5635-5638, 2023.

[10] S. V. Firstov et al., "Laser-active fibers doped with bismuth for a wavelength region of 1.6–1.8 μm," *Quantum Electron.*, vol. 24, no. 5, p. 0902415, 2018.

[11] Y. Wang et al., "Bi-doped optical fibers and fiber amplifiers," *Opt. Mater.: X*, vol. 17, p. 100219, 2023.

[12] Z. Zhai, A. Halder, and J. K. Sahu, "E+S-band bismuth-doped fiber amplifier with 40dB gain and 1.14dB gain per unit length," in *Proc. Eur. Conf. Opt. Commun*., 2023, Paper Th.C.1.1.

[13] I. Razdobreev et al, "Optical properties of Bismuth-doped silica core photonic crystal fiber," *Opt. Exp*., vol. 18, no. 19, pp. 19479-19484, 2010.

[14] A. V. Kharakhordin et al., "Lasing properties of thermally treated $GeO_2$-$SiO_2$ glass fibers doped with bismuth," *Appl. Phys. B*., vol. 126, p. 87, 2020.

[15] V. Fuertes et al., "Tailoring optical properties of bismuth-doped germanosilicate fibers for E/S band amplification," *J. Non-Cryst. Solids*, vol. 613, p. 122381, 2023.

[16] S. V. Firstov et al., "Combined excitation-emission spectroscopy of bismuth active centers in optical fibers," *Opt. Exp*., vol. 19, no. 20, pp. 19551-19561, 2011.

[17] Z. Zhai et al., "Temperature-dependent study on L-band EDFA characteristics pumped at 980 nm and 1480 nm in phosphorus and aluminum-rich erbium-doped silica fibers," *J. Light. Technol.*, vol. 40, no. 14, pp. 4819–4824, 2022.